Coastline, Alofi

Chapter 9
Niue

Introduction

This chapter provides a brief description of Niue, its past and present climate as well as projections for the future. The climate observation network and the availability of atmospheric and oceanic data records are outlined. The annual mean climate, seasonal cycles and the influences of large-scale climate features such as the South Pacific Convergence Zone and patterns of climate variability (e.g. the El Niño-Southern Oscillation) are analysed and discussed. Observed trends and analysis of air temperature, rainfall, extreme events (including tropical cyclones), sea-surface temperature, ocean acidification and mean sea level are presented. Projections for air and sea-surface temperature, rainfall, sea level, ocean acidification and extreme events for the 21st century are provided. These projections are presented along with confidence levels based on expert judgement by Pacific Climate Change Science Program (PCCSP) scientists. The chapter concludes with a summary table of projections (Table 9.3). Important background information including an explanation of methods and models is provided in Chapter 1. For definitions of other terms refer to the Glossary.

9.1 Climate Summary

9.1.1 Current Climate

- Niue has a tropical maritime climate, with a seasonal range in air temperatures of about 4°C between the warmest and coolest months.
- Niue experiences two distinct seasons: a wet season from November to April and dry season from May to October. The timing of the wet season is influenced by the movement of the South Pacific Convergence Zone.
- Year-to-year variability in Niue's climate is strongly associated with the El Niño-Southern Oscillation.
- Warming trends are evident in both annual and seasonal mean air temperatures at Hanan Airport for the period 1950–2009.
- Annual and seasonal rainfall trends for Hanan Airport for the period 1950–2009 are not statistically significant.
- The sea-level rise near Niue measured by satellite altimeters since 1993 is about 5 mm per year.

- On average, Niue experiences 15 tropical cyclones per decade, with most occurring between November and April. The high interannual variability of tropical cyclone numbers makes it difficult to identify any long-term trends in frequency.

9.1.2 Future Climate

Over the course of the 21st century:

- Surface air temperature and sea-surface temperature are projected to continue to increase (*very high* confidence).
- Wet season and annual mean rainfall is projected to increase (*moderate* confidence).
- Little change is projected in dry season rainfall (*low* confidence).
- The intensity and frequency of days of extreme heat are projected to increase (*very high* confidence).
- The intensity and frequency of days of extreme rainfall are projected to increase (*high* confidence).

- Little change is projected in the incidence of drought (*low* confidence).
- Tropical cyclone numbers are projected to decline in the south-east Pacific Ocean basin (0–40ºS, 170ºE–130ºW) (*moderate* confidence).
- Ocean acidification is projected to continue (*very high* confidence).
- Mean sea-level rise is projected to continue (*very high* confidence).

9.2 Country Description

Niue is located in the western South Pacific Ocean and lies at 19°S and 169°W. The island is a raised coral atoll with three reef terraces; the highest terrace averages 69 m above sea level. The land area is 259 km² and the Exclusive Economic Zone has an area of 390 000 km². In addition to the main island, two reef atolls, Antiope and Beveridge, are located within its Exclusive Economic Zone. These are visible only at low tide. The capital of Niue is Alofi (Niue's First National Communication under the UNFCCC, 2000; Niue's Pacific Adaptation to Climate Change, 2006). The estimated population in 2010 was 1470 (Niue Country Statistics, SOPAC, 2010).

There is subsistence agriculture with some small-scale raising of livestock. There are small factories to process passionfruit, lime oil, honey, and coconut cream, and vanilla is being developed as an export crop (Niue's Pacific Adaptation to Climate Change, 2006). There is a very small tourism industry.

Figure 9.1: Niue

9.3 Data Availability

There are currently two operational meteorological observation stations on Niue. The primary station, where multiple observations are conducted on a daily basis, is located at Hanan Airport, south of Alofi on the western side of the island (Figure 9.1). A single daily observation rainfall station is located at Liku on the eastern side of the island. Observations began at Liku in 1990.

A composite record for Hanan Airport, Alofi and Kaimiti has been used.

Observations were taken at Alofi from 1905–1971 and 1977–1996. Between 1971 and 1976 observations were taken at Kaimiti, 2.4 km south of Alofi. The Hanan Airport-Alofi-Kaimiti rainfall and air temperature composite records from 1950–2009 are homogeneous and more than 99% complete.

There are no tide gauge data available for Niue. The Rarotonga (Cook Islands) gauge is the closest available and has been used. Both satellite (from 1993) and in situ sea-level data (1950–2009; termed reconstructed sea level; Volume 1, Section 2.2.2.2) are available on a global 1° x 1° grid.

Long-term locally-monitored sea-surface temperature data are unavailable for Niue, so large-scale gridded sea-surface temperature datasets have been used (HadISST, HadSST2, ERSST and Kaplan Extended SST V2; Volume 1, Table 2.3).

9.4 Seasonal Cycles

Niue has a tropical maritime climate with an average mean temperature of 24°C at Hanan Airport and a seasonal range of just over 4°C between the warmest months (February and March) and the coolest months (July and August) (Figure 9.2). Being a small island, monthly air temperatures in Niue are closely linked to the sea-surface temperatures surrounding the island.

Niue experiences two distinct seasons: a wet season from November to April when the South Pacific Convergence Zone (SPCZ) is closest to the island, and a dry season from May to October when the SPCZ is occasionally inactive and displaced north-eastward. Average annual rainfall for Hanan Airport is 2052 mm.

Niue's climate is also influenced by sub-tropical high pressure systems and trade winds, which blow mainly from the south-east.
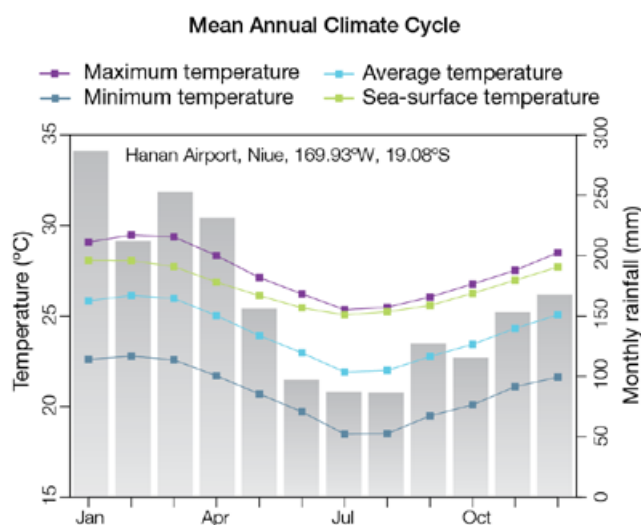

Figure 9.2: Mean annual cycle of rainfall (grey bars) and daily maximum, minimum and mean air temperatures at Hanan Airport, and local sea-surface temperatures derived from the HadISST dataset (Volume 1, Table 2.3).

9.5 Climate Variability

Year-to-year variability in Niue's climate is strongly associated with the El Niño-Southern Oscillation (ENSO). Annual rainfall in the wettest years can be almost four times the rainfall in the driest years. Severe droughts have occurred, with dry season rainfall less than 400 mm, received in 1983, 1991 and 1998, compared with the mean of about 700 mm. The influence of ENSO can be seen in the strong correlation coefficients between Hanan rainfall and ENSO indices (Table 9.1). El Niño events tend to bring below average rainfall, particularly in the wet season, but also cooler conditions during the dry season. The drier conditions in El Niño years are often caused by the SPCZ moving away to the north-east, while in La Niña years the SPCZ moves south-east, bringing more rainfall. ENSO Modoki events (Volume 1, Section 3.4.1) only seem to have an influence on wet season rainfall, but the drier El Niño Modoki and wetter La Niña Modoki events have less of an impact than canonical ENSO events.

Interdecadal variability can be seen in both air temperatures and rainfall at Hanan Airport (Figures 9.3 and 9.4) but the only significant correlation with the Interdecadal Pacific Oscillation (IPO, Table 9.1) is with maximum air temperatures in the wet season.

Table 9.1: Correlation coefficients between indices of key large-scale patterns of climate variability and minimum and maximum temperatures (Tmin and Tmax) and rainfall at Hanan Airport. Only correlation coefficients that are statistically significant at the 95% level are shown.

Climate feature/index		Dry season (May-October)			Wet season (November-April)		
		Tmin	Tmax	Rain	Tmin	Tmax	Rain
ENSO	Niño3.4	-0.37	-0.48	-0.33			-0.61
	Southern Oscillation Index	0.30	0.56	0.30			0.62
Interdecadal Pacific Oscillation Index						0.33	
Southern Annular Mode Index							
ENSO Modoki Index							-0.35
Number of years of data		68	69	100	69	69	103

Training in *Pacific Climate Futures*

9.6 Observed Trends

9.6.1 Air Temperature

Warming trends are evident in both annual and seasonal mean air temperatures at Hanan Airport for the period 1950–2009 (Figure 9.3). The strongest trend is in wet season maximum air temperature, which is more than twice that of minimum air temperature for the same season, and maximum air temperature in the dry season (Table 9.2).

9.6.2 Rainfall

Annual and seasonal rainfall trends for Hanan Airport for the period 1950–2009 are not statistically significant (Table 9.2 and Figure 9.4).

9.6.3 Extreme Events

The tropical cyclone season in the Niue region is between November and April. Occurrences outside this period are rare. The tropical cyclone archive for the Southern Hemisphere indicates that between the 1969/70 and 2006/07 seasons, the centre of 63 tropical cyclones passed within approximately 400 km of Alofi. This represents an average of 15 cyclones per decade. Tropical cyclones were most frequent in El Niño years (19 per decade) and least frequent in La Niña years (9 per decade). The ENSO-neutral average is 15 cyclones per decade. The interannual variability in the number of tropical cyclones in the vicinity of Alofi is large, ranging from zero in some seasons to five in the 1981/82 and 2002/03 seasons (Figure 9.5). This high variability makes it difficult to identify any long-term trends in frequency of tropical cyclones.
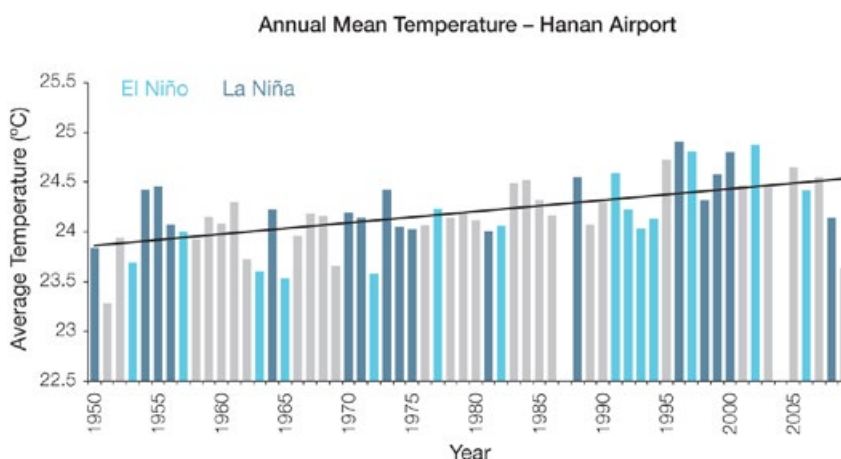

Figure 9.3: Annual mean air temperature at Hanan Airport. Light blue, dark blue and grey bars denote El Niño, La Niña and neutral years respectively.

Table 9.2: Annual and seasonal trends in maximum, minimum and mean air temperature (Tmax, Tmin and Tmean) and rainfall at Hanan Airport for the period 1950–2009. Asterisks indicate significance at the 95% level. Persistence is taken into account in the assessment of significance as in Power and Kociuba (in press). The statistical significance of the air temperature trends is not assessed.

	Hanan Airport Tmax (°C per 10 yrs)	Hanan Airport Tmin (°C per 10 yrs)	Hanan Airport Tmean (°C per 10 yrs)	Hanan Airport Rain (mm per 10 yrs)
Annual	+0.15	+0.08	+0.11	+25
Wet season	+0.21	+0.08	+0.15	+4
Dry season	+0.09	+0.09	+0.10	+24

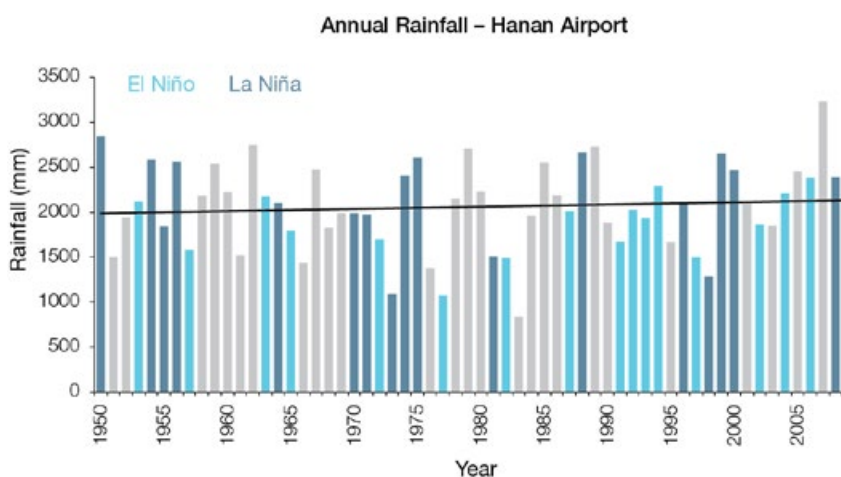**Figure 9.4:** Annual rainfall at Hanan Airport. Light blue, dark blue and grey bars denote El Niño, La Niña and neutral years respectively.

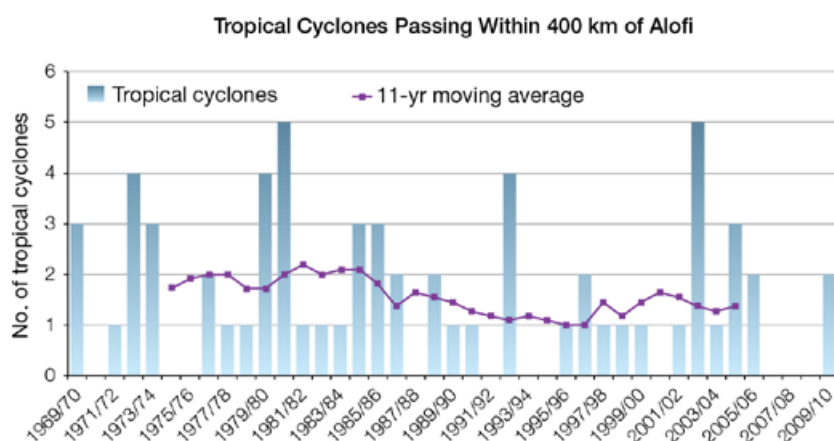**Tropical Cyclones Passing Within 400 km of Alofi**

Figure 9.5: Tropical cyclones passing within 400 km of Alofi per season. The 11-year moving average is in purple.

Niue's economy suffered significantly from high winds, storm surge and intense rainfall associated with Tropical Cyclone Heta on 4 January 2004. In total, the storm caused over NZ$37.7 million damage, three times Niue's Gross Domestic Product.

Agriculture is very important to the lifestyle of Niueans and the economy. Nearly all households have plantations of taro. These gardens are mainly rain-fed, making them prone to El Niño associated drought. Conversely, Niue is occasionally affected by prolonged periods of above normal rainfall associated with La Niña, which can result in outbreaks of yam disease (*Yam anthranose*) and mosquito-borne diseases such as dengue fever.

9.6.4 Sea-Surface Temperature

Historical sea-surface temperature changes around Niue show considerable decadal variability. Water temperatures declined slightly around the island from the 1950s to the late 1980s. This was followed by a period of warming (approximately 0.08°C per decade for 1970–present). Figure 9.7 shows the 1950–2000 sea-surface temperature changes (relative to a reference year of 1990) from three different large-scale sea-surface temperature gridded datasets (HadSST2, ERSST and Kaplan Extended SST V2; Volume 1, Table 2.3). At these regional scales, natural variability plays a large role in determining sea-surface temperature, making it difficult to identify long-term trends.

9.6.5 Ocean Acidification

Based the large-scale distribution of coral reefs across the Pacific and the seawater chemistry, Guinotte et al. (2003) suggested that seawater aragonite saturation states above 4 were optimal for coral growth and for the development of healthy reef ecosystems, with values from 3.5 to 4 adequate for coral growth, and values between 3 and 3.5, marginal. Coral reef ecosystems were not found at seawater aragonite saturation states below 3 and these conditions were classified as extremely marginal for supporting coral growth.

In the Niue region, the aragonite saturation state has declined from about 4.5 in the late 18th century to an observed value of about 4.0 ± 0.1 by 2000.

9.6.6 Sea Level

Monthly averages of the historical tide gauge (Rarotonga, Cook Islands; 1977–2001 and 1993–present), satellite (since 1993) and gridded sea-level (since 1950) data agree well after 1993 and indicate interannual variability in sea levels of about 17 cm (estimated 5–95% range) after removal of the seasonal cycle (Figure 9.9). The sea-level rise near Niue measured by satellite altimeters (Figure 9.6) since 1993 is about 5 mm per year, larger than the global average of 3.2 ± 0.4 mm per year. This rise is part of a pattern related to climate variability from year to year and decade to decade (Figure 9.9).

9.6.7 Extreme Sea-Level Events

As there is no tide gauge in Niue, this analysis could not be undertaken.

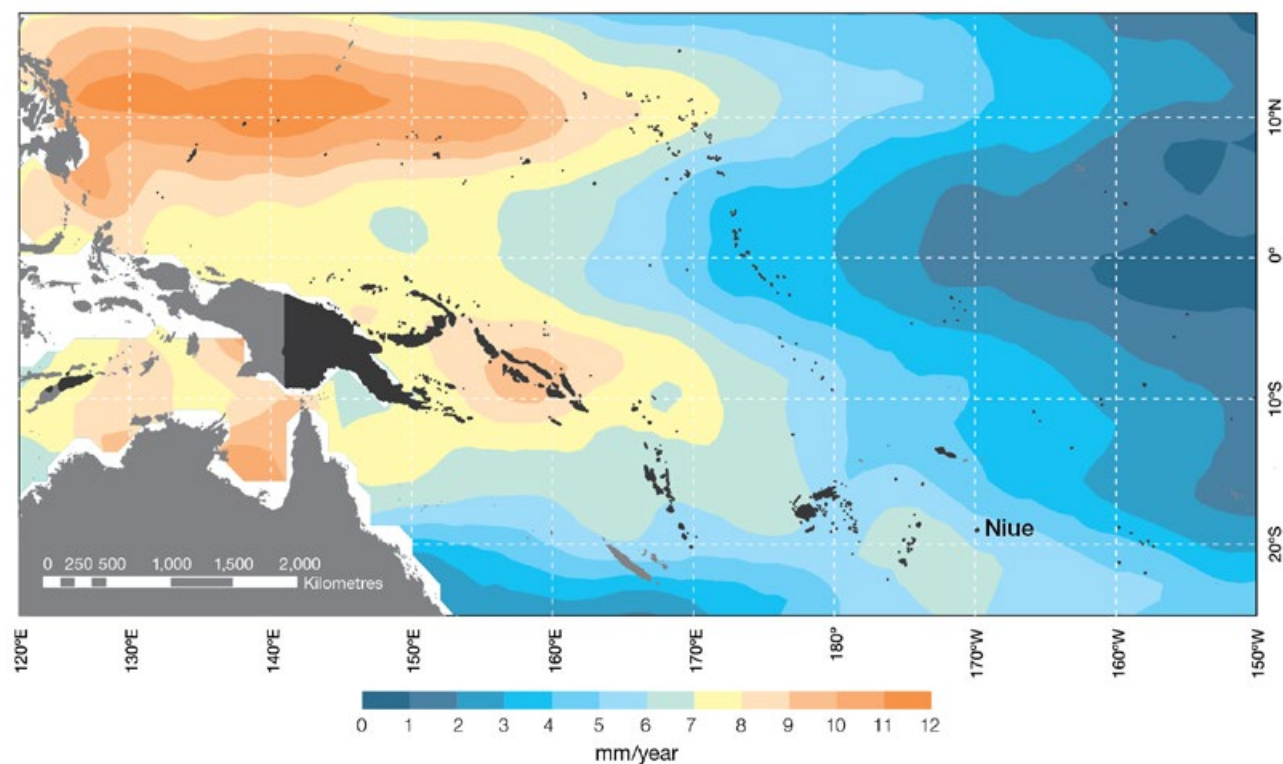Regional Distribution of the Rate of Sea-Level Rise

Figure 9.6: The regional distribution of the rate of sea-level rise measured by satellite altimeters from January 1993 to December 2010, with the location of Niue indicated. Further information on regional distribution of sea-level rise is provided in Volume 1, Section 3.6.3.2.

9.7 Climate Projections

Climate projections have been derived from up to 18 global climate models from the CMIP3 database, for up to three emissions scenarios (B1 (low), A1B (medium) and A2 (high)) and three 20-year periods (centred on 2030, 2055 and 2090, relative to 1990). These models were selected based on their ability to reproduce important features of the current climate (Volume 1, Section 5.2.3) so projections from each of the models are plausible representations of the future climate. This means there is not one single projected future for Niue, but rather a range of possible futures. The full range of these futures is discussed in the following sections.

These projections do not represent a value specific to any actual location, such as a town in Niue. Instead, they refer to an average change over the broad geographic region encompassing Niue and the surrounding ocean (Figure 1.1 shows the regional boundaries). Section 1.7 provides important information about interpreting climate model projections.

9.7.1 Temperature

Surface air temperature and sea-surface temperature are projected to continue to increase over the course of the 21st century. There is *very high* confidence in this direction of change because:

- Warming is physically consistent with rising greenhouse gas concentrations.
- All CMIP3 models agree on this direction of change.

The majority of CMIP3 models simulate a slight increase (<1°C) in annual and seasonal mean temperature by 2030, however by 2090 under the A2 (high) emissions scenario temperature increases of greater than 2.5°C are simulated by almost all models (Table 9.3). Given the close relationship between surface air temperature and sea-surface temperature, a similar (or slightly weaker) rate of warming is projected for the surface ocean (Figure 9.7).

There is *moderate* confidence in this range and distribution of possible futures because:

- There is generally a large discrepancy between modelled and observed temperature trends over the past 50 years in the vicinity of Niue, although this may be partly due to limited observational records (Figure 9.7).

Interannual variability in surface air temperature and sea-surface temperature over Niue is strongly influenced by ENSO in the current climate (Section 9.5). As there is no consistency in projections of future ENSO activity (Volume 1, Section 6.4.1) it is not possible to determine whether interannual variability in temperature will change in the future. However, ENSO is expected to continue to be an important source of variability for the region.

9.7.2 Rainfall

Wet Season (November-April)

Wet season rainfall is projected to increase over the course of the 21st century. There is *moderate* confidence in this direction of change because:

- An increase in wet season rainfall is consistent with the projected likely increase intensity of the South Pacific Convergence Zone (SPCZ), which lies over Niue in this season (Volume 1, Section 6.4.5).
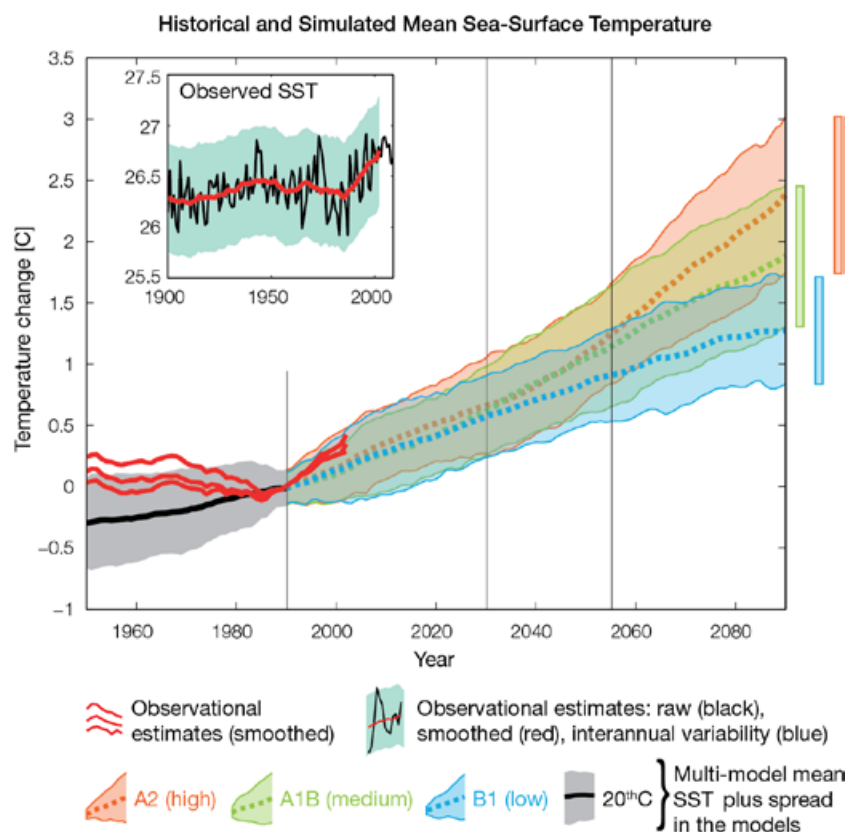

Historical and Simulated Mean Sea-Surface Temperature

Figure 9.7: Historical climate (from 1950 onwards) and simulated historical and future climate for annual mean sea-surface temperature (SST) in the region surrounding Niue, for the CMIP3 models. Shading represents approximately 95% of the range of model projections (twice the inter-model standard deviation), while the solid lines represent the smoothed (20-year running average) multi-model mean temperature. Projections are calculated relative to the 1980–1999 period (which is why there is a decline in the inter-model standard deviation around 1990). Observational estimates in the main figure (red lines) are derived from the HadSST2, ERSST and Kaplan Extended SST V2 datasets (Volume 1, Section 2.2.2). Annual average (black) and 20-year running average (red) HadSST2 data is also shown inset.

- The majority of CMIP3 models agree on this direction of change by 2090.

The majority of CMIP3 models simulate little change (-5% to 5%) in wet season rainfall by 2030, however by 2090 the majority simulate an increase (>5%), with approximately one third simulating a large increase (>15%) under the A2 (high) emissions scenario (Table 9.3). There is *moderate* confidence in this range and distribution of possible futures because:

- In simulations of the current climate, the CMIP3 models generally locate the SPCZ in the correct location relative to Niue in the wet season (Brown et al., 2011).
- The CMIP3 models are unable to resolve many of the physical processes involved in producing rainfall. As a consequence, they do not simulate rainfall as well as other variables such as temperature (Volume 1, Chapter 5).

Dry Season (May-October)

Little change is projected in dry season rainfall over the course of the 21st century. There is *low* confidence in this direction of change because:

- There is little agreement amongst the models, with approximately equal numbers simulating an increase (>5%), decrease (<-5%) or little change (-5% to 5%) by 2090 across the B1 (low), A1B (medium) and A2 (high) emissions scenarios.
- In simulations of the current climate, some CMIP3 models have an SPCZ that extends too far east during the dry season, with too much rainfall over Niue (Brown et al., 2011).
- The CMIP3 models are unable to resolve many of the physical processes involved in producing rainfall.

Annual

Total annual rainfall is projected to increase over the course of the 21st century. There is *moderate* confidence in this direction of change because:

- Approximately half (A1B (medium) emissions scenario) and the majority (A2 (high) emissions scenario)

of CMIP3 models agree on this direction of change by 2090.

- There is moderate and low confidence in wet and dry season rainfall projections respectively, as discussed above.

Interannual variability in rainfall over Niue is strongly influenced by ENSO in the current climate, via the movement of the SPCZ (Section 9.5). As there is no consistency in projections of future ENSO activity (Volume 1, Section 6.4.1) it is not possible to determine whether interannual variability in rainfall will change in the future.

9.7.3 Extremes

Temperature

The intensity and frequency of days of extreme heat are projected to increase over the course of the 21st century. There is *very high* confidence in this direction of change because:

- An increase in the intensity and frequency of days of extreme heat is physically consistent with rising greenhouse gas concentrations.
- All CMIP3 models agree on the direction of change for both intensity and frequency.

The majority of CMIP3 models simulate an increase of approximately 1°C in the temperature experienced on the 1-in-20-year hot day by 2055 under the B1 (low) emissions scenario, with an increase of over 2.5°C simulated by the majority of models by 2090 under the A2 (high) emissions scenario (Table 9.3). There is *low* confidence in this range and distribution of possible futures because:

- In simulations of the current climate, the CMIP3 models tend to underestimate the intensity and frequency of days of extreme heat (Volume 1, Section 5.2.4).
- Smaller increases in the frequency of days of extreme heat are projected by the CCAM 60 km simulations.

Rainfall

The intensity and frequency of days of extreme rainfall are projected to

increase over the course of the 21st century. There is *high* confidence in this direction of change because:

- An increase in the frequency and intensity of extreme rainfall is consistent with larger-scale projections, based on the physical argument that the atmosphere is able to hold more water vapour in a warmer climate (Allen and Ingram, 2002; IPCC, 2007). It is also consistent with the projected likely increase in SPCZ intensity (Volume 1, Section 6.4.5).
- Almost all of the CMIP3 models agree on this direction of change for both intensity and frequency.

The majority of CMIP3 models simulate an increase of at least 5 mm in the amount of rain received on the 1-in-20-year wet day by 2055 under the B1 (low) emissions scenario, with an increase of at least 25 mm simulated by 2090 under the A2 (high) emissions scenario. The majority of models project that the current 1-in-20-year extreme rainfall event will occur, on average, two to three times per 20-year period by 2055 under the B1 (low) emissions scenario and three to four times per 20-year period by 2090 under the A2 (high) emissions scenario. There is *low* confidence in this range and distribution of possible futures because:

- In simulations of the current climate, the CMIP3 models tend to underestimate the intensity and frequency of extreme rainfall (Volume 1, Section 5.2.4).
- The CMIP3 models are unable to resolve many of the physical processes involved in producing extreme rainfall.

Drought

Little change is projected in the incidence of drought over the course of the 21st century. There is *low* confidence in this direction of change because:

- There is only low confidence in the range of dry season rainfall projections (Section 9.7.2), which

directly influences projections of future drought conditions.

The majority of CMIP3 models project that the frequency of mild drought will remain approximately stable at six to seven times every 20 years, under all emissions scenarios. The frequency of moderate and severe drought is also projected to remain stable, at once to twice and once every 20 years, respectively

Tropical Cyclones

Tropical cyclone numbers are projected to decline in the south-east Pacific Ocean basin (0–40ºS, 170ºE–130ºW) over the course of the 21st century. There is *moderate* confidence in this direction of change because:

- Many studies suggest a decline in tropical cyclone frequency globally (Knutson et al., 2010).
- Tropical cyclone numbers decline in the south-east Pacific Ocean in the majority assessment techniques.

Based on the direct detection methodologies (Curvature Vorticity Parameter (CVP) and the CSIRO Direct Detection Scheme (CDD) described in Volume 1, Section 4.8.2), 65% of projections show no change or a decrease in tropical cyclone formation when applied to the CMIP3 climate models for which suitable output is available. When these techniques are applied to CCAM, 100% of projections show a decrease in tropical cyclone formation. In addition, the Genesis Potential Index (GPI) empirical technique suggests that conditions for tropical cyclone formation will become less favourable in the south-east Pacific Ocean basin, for all analysed CMIP3 models. There is moderate confidence in this range and distribution of possible futures because in simulations of the current climate, the CVP, CDD and GPI methods capture the frequency of tropical cyclone activity reasonably well (Volume 1, Section 5.4).
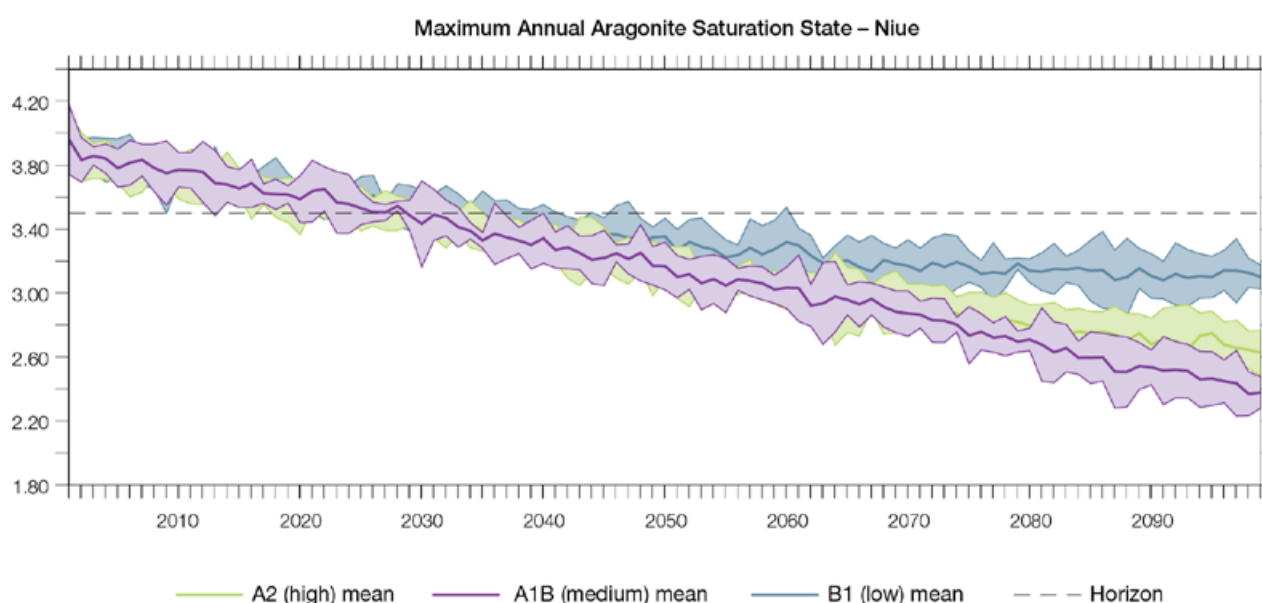
Despite this projected reduction in total cyclone numbers, five of the six CCAM 60 km simulations show an increase in the proportion of the most severe cyclones. Most models also indicate a reduction in tropical cyclone wind hazard north of 20ºS latitude and regions of increased hazard south of 20ºS latitude. This increase in wind hazard coincides with a poleward shift in the latitude at which tropical cyclones are most intense.

9.7.4 Ocean Acidification

The acidification of the ocean will continue to increase over the course of the 21st century. There is *very high* confidence in this projection as the rate of ocean acidification is driven primarily by the increasing oceanic uptake of carbon dioxide, in response to rising atmospheric carbon dioxide concentrations.

Projections from all analysed CMIP3 models indicate that the annual maximum aragonite saturation state will reach values below 3.5 by about 2040 and continue to decline thereafter (Figure 9.8; Table 9.3). There is *moderate* confidence in this range and distribution of possible futures because the projections are based on climate models without an explicit representation of the carbon cycle and with relatively low resolution and known regional biases.

Maximum Annual Aragonite Saturation State – Niue

The impact of acidification change on the health of reef ecosystems is likely to be compounded by other stressors including coral bleaching, storm damage and fishing pressure.

Figure 9.8: Multi-model projections, and their associated uncertainty (shaded area represents two standard deviations), of the maximum annual aragonite saturation state in the sea surface waters of Niue under the different emissions scenarios. The dashed black line represents an aragonite saturation state of 3.5.

9.7.5 Sea Level

Mean sea level is projected to continue to rise over the course of the 21st century. There is *very high* confidence in this direction of change because:

- Sea-level rise is a physically consistent response to increasing ocean and atmospheric temperatures, due to thermal expansion of the water and the melting of glaciers and ice caps.

- Projections arising from all CMIP3 models agree on this direction of change.

The CMIP3 models simulate a rise of between approximately 5–15 cm by 2030, with increases of 20–60 cm indicated by 2090 under the higher emissions scenarios (i.e. A2 (high) and A1B (medium); Figure 9.9; Table 9.3). There is *moderate* confidence in this range and distribution of possible futures because:

- There is significant uncertainty surrounding ice-sheet contributions to sea-level rise and a rise larger than projected above cannot be excluded (Meehl et al., 2007b). However, understanding of the processes is currently too limited to provide a best estimate or an upper bound (IPCC, 2007).

- Globally, since the early 1990s, sea level has been rising near the upper end of the above projections. During the 21st century, some studies (using semi-empirical models) project faster rates of sea-level rise.

Interannual variability of sea level will lead to periods of lower and higher regional sea levels. In the past, this interannual variability has been about 17 cm (5–95% range, after removal of the seasonal signal; dashed lines in Figure 9.9 (a)) and it is likely that a similar range will continue through the 21st century. In addition, winds and waves associated with weather phenomena will continue to lead to extreme sea-level events.

In addition to the regional variations in sea level associated with ocean and mass changes, there are ongoing changes in relative sea level associated with changes in surface loading over the last glacial cycle (glacial isostatic adjustment) and local tectonic motions. The glacial isostatic motions are relatively small for the PCCSP region.
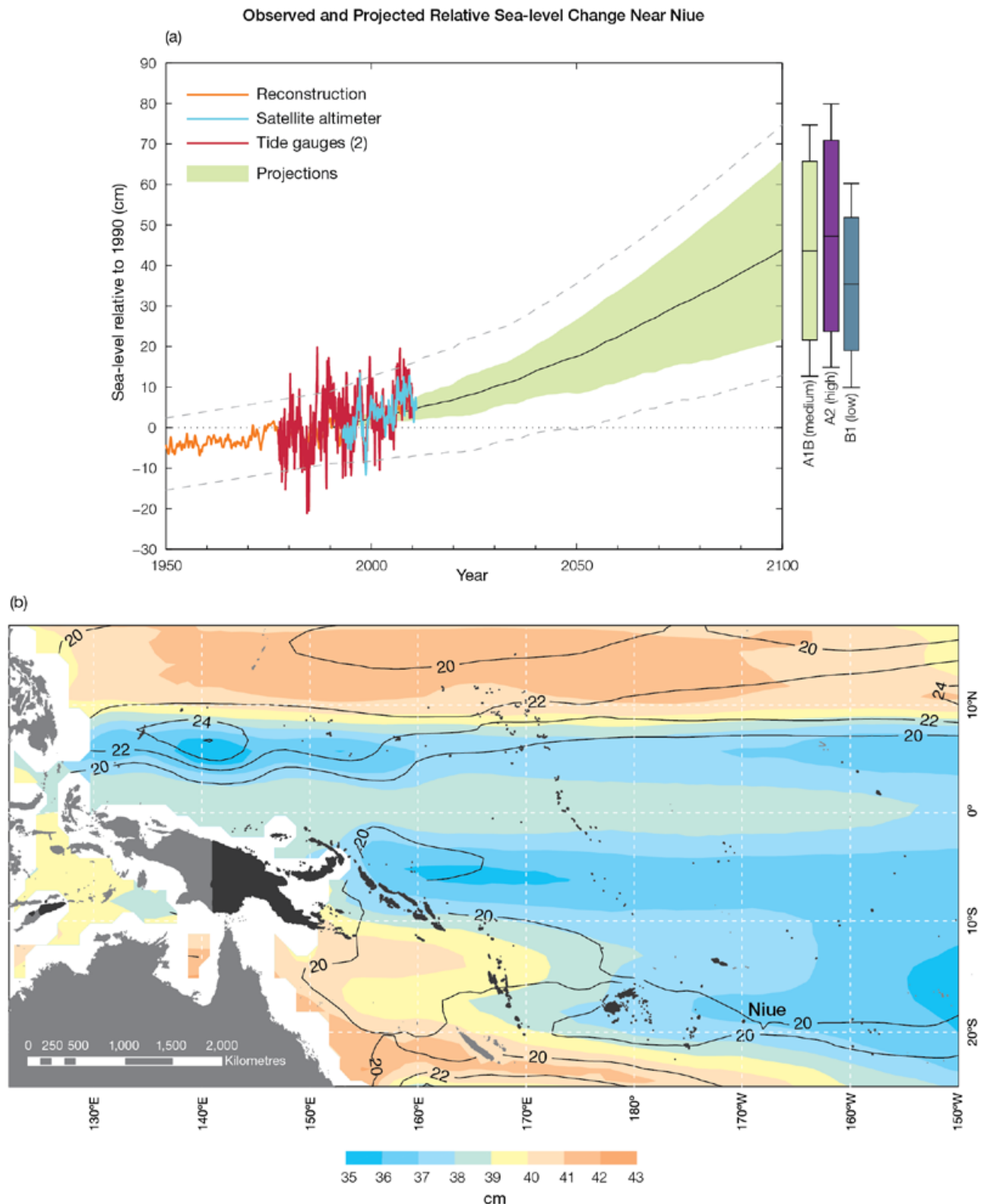
Figure 9.9: Observed and projected relative sea-level change near Niue. (a) The observed in situ relative sea-level records from Rarotonga (Cook Islands) are indicated in red, with the satellite record (since 1993) in light blue. The gridded sea level at Niue (since 1950, from Church and White (in press)) is shown in orange. The projections for the A1B (medium) emissions scenario (5–95% uncertainty range) are shown by the green shaded region from 1990–2100. The range of projections for the B1 (low), A1B (medium) and A2 (high) emissions scenarios by 2100 are also shown by the bars on the right. The dashed lines are an estimate of interannual variability in sea level (5–95% range about the long-term trends) and indicate that individual monthly averages of sea level can be above or below longer-term averages. (b) The projections (in cm) for the A1B (medium) emissions scenario in the Niue region for the average over 2081–2100 relative to 1981–2000 are indicated by the shading, with the estimated uncertainty in the projections indicated by the contours (in cm).

9.7.6 Projections Summary

The projections presented in Section 9.7 are summarised in Table 9.3. For detailed information regarding the various uncertainties associated with the table values, refer to the preceding text in Sections 9.7 and 1.7, in addition to Chapters 5 and 6 in Volume 1. When interpreting the differences between projections for the B1 (low), A1B (medium) and A2 (high) emissions scenarios, it is also important to consider the emissions pathways associated with each scenario (Volume 1, Figure 4.1) and the fact that a slightly different subset of models was available for each (Volume 1, Appendix 1).

Table 9.3: Projected change in the annual and seasonal mean climate for Niue, under the B1 (low; blue), A1B (medium; green) and A2 (high; purple) emissions scenarios. Projections are given for three 20-year periods centred on 2030 (2020–2039), 2055 (2046–2065) and 2090 (2080–2099), relative to 1990 (1980–1999). Values represent the multi-model mean change ± twice the inter-model standard deviation (representing approximately 95% of the range of model projections), except for sea level where the estimated mean change and the 5–95% range are given (as they are derived directly from the Intergovernmental Panel on Climate Change Fourth Assessment Report values). The confidence (Section 1.7.2) associated with the range and distribution of the projections is also given (indicated by the standard deviation and multi-model mean, respectively). See Volume 1, Appendix 1 for a complete listing of CMIP3 models used to derive these projections.

Variable	Season	2030	2055	2090	Confidence
Surface air temperature (°C)	Annual	+0.6 ± 0.4	+1.0 ± 0.5	+1.3 ± 0.6	Moderate
		+0.7 ± 0.5	+1.3 ± 0.6	+2.0 ± 0.8	
		+0.7 ± 0.4	+1.3 ± 0.4	+2.5 ± 0.7	
Maximum temperature (°C)	1-in-20-year event	N/A	+1.0 ± 0.7	+1.2 ± 0.7	Low
			+1.4 ± 0.6	+2.0 ± 1.0	
			+1.5 ± 0.6	+2.6 ± 1.4	
Minimum temperature (°C)	1-in-20-year event	N/A	+1.2 ± 1.7	+1.4 ± 1.8	Low
			+1.5 ± 1.6	+1.9 ± 2.0	
			+1.5 ± 1.7	+2.2 ± 1.7	
Total rainfall (%)*	Annual	+2 ± 15	+2 ± 11	+5 ± 13	Moderate
		+1 ± 12	+5 ± 14	+5 ± 13	
		+5 ± 12	+6 ± 13	+10 ± 20	
Wet season rainfall (%)*	November-April	+3 ± 15	+3 ± 14	+6 ± 19	Moderate
		+1 ± 12	+6 ± 15	+8 ± 17	
		+5 ± 13	+7 ± 17	+14 ± 20	
Dry season rainfall (%)*	May-October	+1 ± 17	0 ± 13	+3 ± 16	Low
		+3 ± 21	+3 ± 21	+2 ± 22	
		+5 ± 13	+5 ± 17	+4 ± 30	
Sea-surface temperature (°C)	Annual	+0.6 ± 0.3	+0.9 ± 0.4	+1.3 ± 0.4	Moderate
		+0.6 ± 0.4	+1.1 ± 0.5	+1.9 ± 0.6	
		+0.7 ± 0.4	+1.3 ± 0.4	+2.4 ± 0.6	
Aragonite saturation state (Ωar)	Annual maximum	+3.5 ± 0.1	+3.2 ± 0.1	+3.1 ± 0.1	Moderate
		+3.4 ± 0.1	+3.0 ± 0.1	+2.7 ± 0.2	
		+3.4 ± 0.1	+3.0 ± 0.1	+2.5 ± 0.2	
Mean sea level (cm)	Annual	+10 (5–16)	+18 (10–27)	+32 (17–46)	Moderate
		+10 (5–15)	+20 (10–30)	+38 (19–57)	
		+10 (4–17)	+20 (10–30)	+40 (20–60)	

*The MIROC3.2(medres) and MIROC3.2(hires) models were eliminated in calculating the rainfall projections, due to their inability to accurately simulate present-day activity of the South Pacific Convergence Zone (Volume 1, Section 5.5.1).